Evolutionarily conserved IL-20 enhances the response of JAK1/STAT3 axis in *Carassius cuvieri* × *Carassius auratus* red var

Qiongyao Zeng [1], Niewen Hu [1], Zhengwei Li, Ye Yang, Zejun Zhou [*]

State Key Laboratory of Developmental Biology of Freshwater Fish, College of Life Sciences, Hunan Normal University, Changsha, 410081, China

A B S T R A C T

The IL-20 cytokine family, which includes only IL-20, IL-22 and IL-26 in teleost, has a wide range of biological functions and is essential for epithelial integrity and innate host defense. IL-22 and IL-26 are the most intensively studied cytokine within this family; however, the immunological function of IL-20 in fish is essentially unknown. In this study, we examined the expression and function of an IL-20 homologue (WR-IL20) from White crucian carp (*Carassius cuvieri*, WCC, female) × Red crucian carp (*Carassius auratus* red var., RCC, male). WR-IL20 and its parents, WCC-IL20 and RCC-IL20, were both composed of 177 residues with high identities among them. Additionally, gene structure, functional domain, tertiary structure, multiple sequence alignment, and phylogeny analysis showed a conserved status between WR-IL20, WCC-IL20 and RCC-IL20. WR-IL20, WCC-IL20 and RCC-IL20 were mainly expressed in the head kidney and were upregulated by *Aeromonas hydrophila* infection *in vivo*. Furthermore, recombinant WR-IL20 protein (rWR-IL20) induced increased transcript levels of *c-Myc*, *cyclin D*, *Bcl-2*, *JAK1*, *TYK2* and *STAT3* in head kidney lymphocytes *in vitro*. These results provide a new perspective for understanding the origin, evolution and function of IL-20 in teleost.

1. Introduction

Interleukin (IL) 20 belongs to the IL-20 subfamily that comprises IL-19, IL-22, IL-24 and IL-26 which are members of a large IL-10 super-family [1,2]. It has been shown that monocytes, macrophages, kerati-nocytes (23), and dendritic cells can secrete IL-20 [3]. In addition, stimulation with LPS, IL-1β, IL-8, IL-17, IL-22 and TNF-α could induce IL-20 expression in these epithelial cells and myeloid cells [4]. Furthermore, infection of mice with pathogen *Citrobacter rodentium* leads to increased IL-20 expression [5]. Increased expression of IL-20 has been reported in biopsies of patients with ulcerative colitis and Crohn's disease [6].

In mammals, IL-20 is a pleiotropic cytokine that has a potent in-flammatory, chemoattractant, and antigenic characteristic features [7]. The mechanism would be mediated by two types of receptors, type I receptor complex and type II receptor complex [2]. The IL-20 type I receptor complex is composed of a heterodimer of IL-20Rα and IL-20Rβ, while type II receptor complex is composed of IL-22Rα and IL-20Rβ [8]. Upon activation, the IL-20 receptors trigger cellular signaling pathways involving the Janus Kinase (JAK) and the signal transducer and activator

of transcription (STAT) and ERK1/2 to elicit cellular responses [1,2]. Besides, IL-20 enhances proliferation and differentiation of epithelium during inflammation, and protects tissues from infection by inducing the production of antimicrobial peptides such as β defensins, S100a8 and lipocalin 2 [5].

In fish, the IL-20 subfamily members only including IL-20 like (IL-20L), IL-22 and IL-26 are present [9–11]. Among these, the IL-20L has been described in *Tetraodon nigroviridis*, *Daino rario*, *Oncorhynchus mykiss*, *Ctenopharyngodon idella* and *Channa argus* [11–16]. For example, the expression of IL-20L in grass carp (*Ctenopharyngodon idella*) is upregulated in the head kidney after infection with *Flavobactrium columnare* and grass carp reovirus II (GCRV II) [11]. Functionally, grass carp IL-20L is shown to be effective in inducing the expressions of Th cytokine genes, macrophage marker genes and inflammatory genes [11].

Carassius cuvieri × *Carassius auratus* red var. (WR, 2n = 100), origi-nated from White crucian carp (*Carassius cuvieri*, WCC, female) × Red crucian carp (*Carassius auratus* red var., RCC, male), has many advan-tages, such as faster growth, better taste and stronger disease resistance compared with the WCC and RCC, and has become an economically
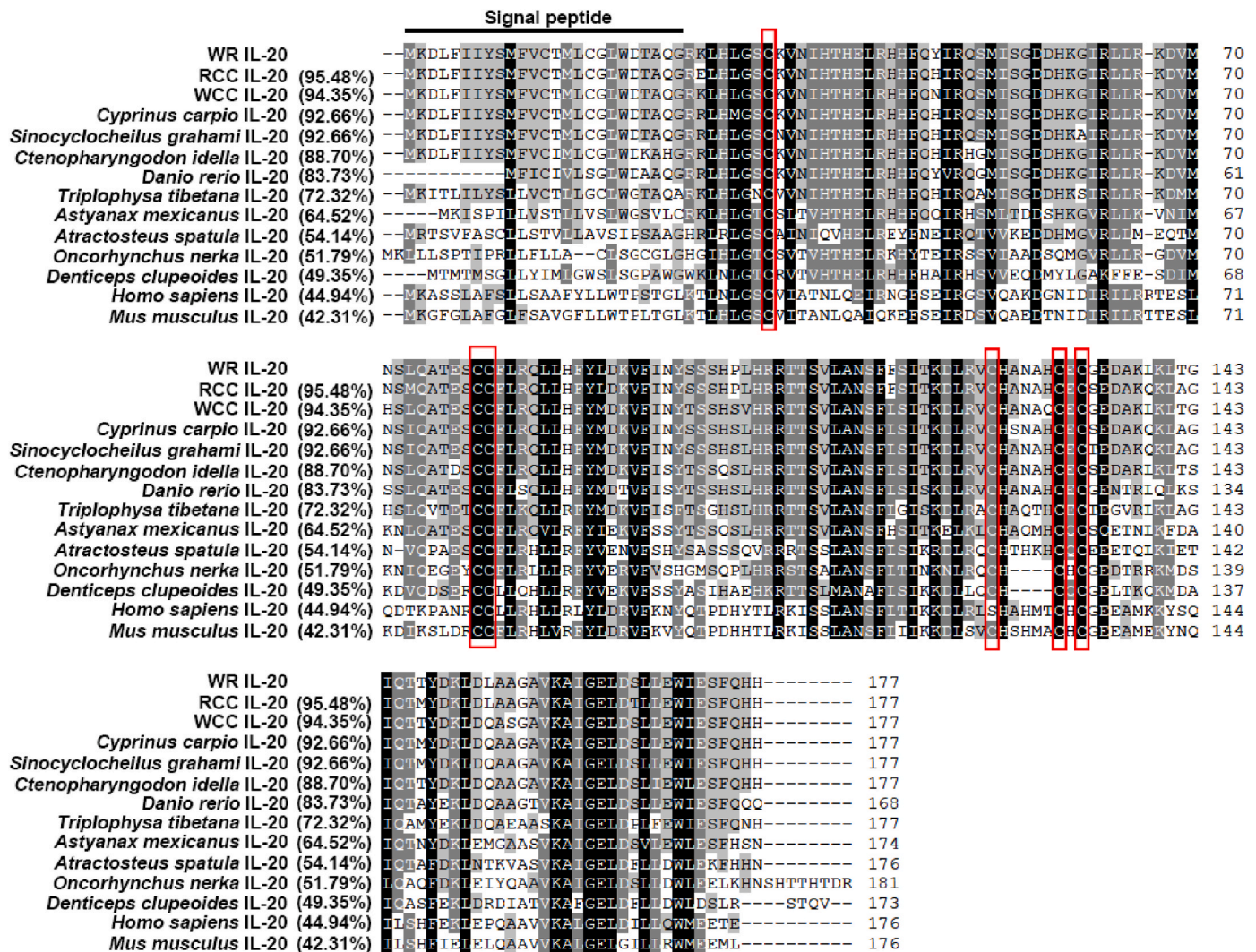
Fig. 1. Sequences of WR-IL20, WCC-IL20 and RCC-IL20. Alignment of the sequences of WR-IL20, WCC-IL20 and RCC-IL20. Numbers in the end of each species indicate overall sequence identities between WR-IL20 and the compared sequences. The consensus residues are in black, the residues that are ≥80% identical among the aligned sequences are in grey. The GenBank accession numbers of the aligned sequences are as follows: WR-IL20, OQ822161; WCC-IL20, OQ822160; RCC-IL20, OQ822159; *Cyprinus carpio*, XP_018961607.1; *Sinocyclocheilus grahami*, XP_016094211.1; *Ctenopharyngodon idella*, XP_051767696.1; *Danio rerio*, NP_001076424.1; *Triplophysa tibetana*, KAA0707760.1; *Astyanax mexicanus*, XP_007247852.3; *Atractosteus spatula*, MBN3324885.1; *Oncorhynchus nerka*, XP_029543883.1; *Denticeps clupeoides*, XP_028854808.1; *Homo sapiens*, AAQ88686.1; *Mus musculus*, NP_067355.1. The signal peptide is labeled by black line. The cysteine residues are labeled by red boxes.

important species cultured in China [17]. However, fish motile aero-monad septicemia (MAS) has caused serious economic losses to the Chinese cyprinid fish industry in recent decades, and *Aeromonas hydrophila* is identified as the etiologic agent of MAS disease outbreaks [18]. In this work, we described an IL-20 homologue from *Carassius cuvieri* × *Carassius auratus* red var. (named WR-IL20), and we compared the differences of phylogenetic status, collinearity, exon-intron composition, tertiary structure and functional motif between WR-IL20 and its parents (WCC-IL20 and RCC-IL20). In addition, we found that the expressions of WR-IL20, WCC-IL20 and RCC-IL20 were upregulated by *A. hydrophila* challenge. Furthermore, we compared the *in vitro* immune effects of WR-IL20 on head kidney leukocytes of WR, WCC and RCC, which may provide the evidence for elucidating the mechanism of heterosis in WR.

2. Materials and methods

2.1. Fish

Healthy WR, WCC and RCC (average 25.5 g) were collected from the Engineering Research Center of Polyploidy Fish Breeding and Reproduction of State Education Ministry in Hunan Normal University. WR, WCC and RCC were acclimatized in 70 × 65 × 65 cm plastic aquarium (25 fish/aquarium) and fed with commercial diet twice a day. During the experiment, the water environment was as follows: temperature was 26.11 ± 1.15 °C, pH was 7.0 ± 0.2, dissolved oxygen was higher than 7.0 mg/L, and natural photoperiod, respectively. Before the experiment, fish were randomly sampled and verified to be absent of bacterial pathogens in liver, kidney, blood and spleen as reported previously [19]. For tissue collection, fish were euthanized with tricaine methanesulfonate (MS222, Sigma, St. Louis, MO, USA) at a concentration of 100 mg/L. We followed the laboratory animal guideline for the ethical review of the animal welfare of China (GB/T 35892–2018). Fish work was approved by the Animal Care Committee of Hunan Normal University
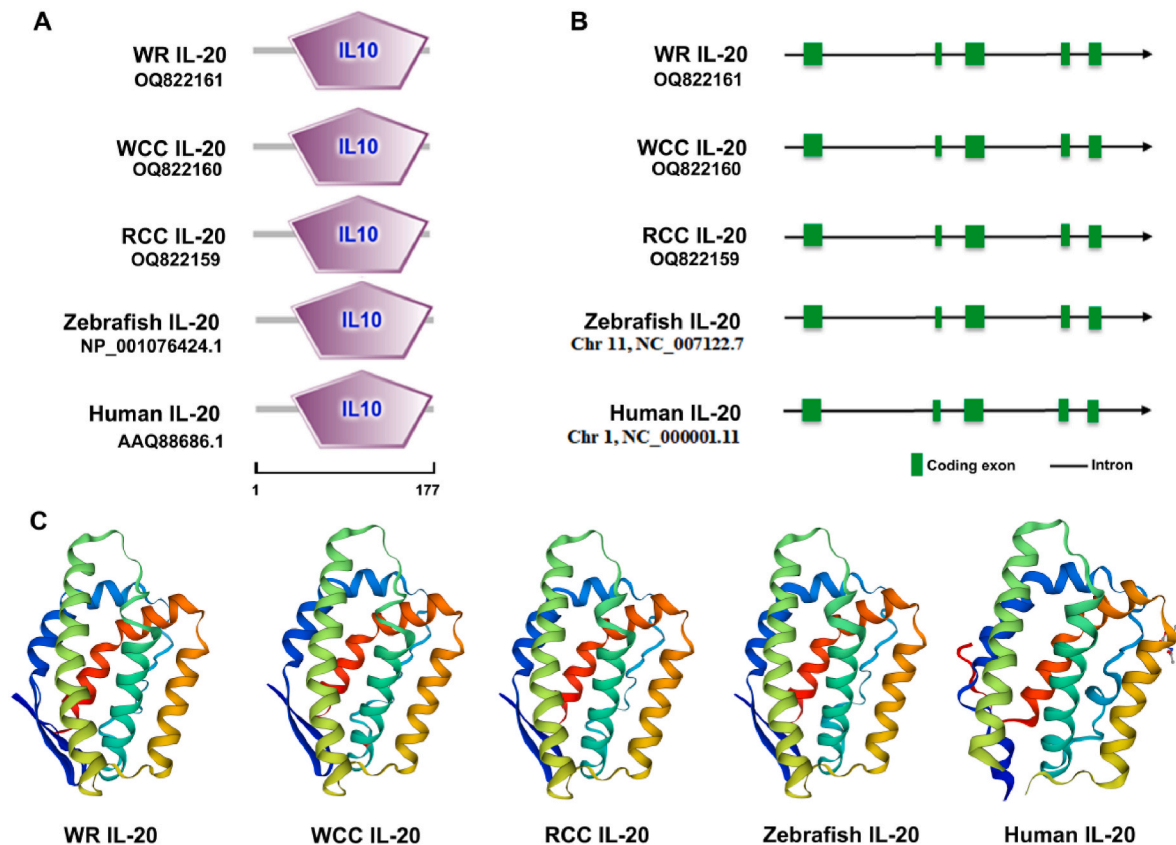
Fig. 2. Gene structure analyses of WR-IL20, WCC-IL20 and RCC-IL20. (A) Predicted domains of WR-IL20, WCC-IL20, RCC-IL20, zebrafish IL-20 and human IL-20. Conserved IL10 domains were shown. (B) Genomic structures of WR-IL20, WCC-IL20, RCC-IL20, zebrafish IL-20 and human IL-20. The green rectangles represent coding exons. The horizontal lines between two rectangles represent introns. (C) Predicted tertiary structures of WR-IL20, WCC-IL20, RCC-IL20, zebrafish IL-20 and human IL-20.

(2023109).

2.2. Cloning of WR-IL20, WCC-IL20 and RCC-IL20

Total RNA from kidney of WR, WCC and RCC were extracted using TRIzol Reagent (Invitrogen, California, CA, USA) as described in the manufacturer's instruction respectively. The first-strand cDNAs from WR, WCC and RCC were synthesized from the total RNA using the Maxima H Minus First Strand cDNA Synthesis Kit with dsDNase (Thermo Fisher Scientific, Waltham, MA, USA) according to the manufacturer's protocol. *WR-IL20*, *WCC-IL20* and *RCC-IL20* were amplified using primers IL20-F1/IL20-R1, respectively (Table S1). The sequences of *WR-IL20*, *WCC-IL20* and *RCC-IL2*0 had been deposited in GenBank database under the accession number OQ822161, OQ822160 and OQ822159, respectively. The DNA templates from WR, WCC and RCC were extracted from kidney by genomic DNA extraction kit (Tiangen biotech., Beijing, China) according to user's manual. The genomic DNA sequences of *WR-IL20*, *WCC-IL20* and *RCC-IL20* were amplified through primers IL20-F1/IL20-R1, respectively (Table S1).

2.3. Sequence, structure and phylogenetic analysis

The cDNA and amino acid sequences of WR-IL20, WCC-IL20 and RCC-IL20 were analyzed using the BLAST program at the National Center for Biotechnology Information (NCBI). Domain search was performed with the simple modular architecture research tool (SMART) version 4.0 and the conserved domain search program of NCBI. The tertiary structures of proteins were predicted by SWISS-MODEL (https://swissmodel.expasy.org/) using Human IL-20 (SMTL ID: 4doh. A) as a template. Multiple sequence alignments were created with

Clustal X. Phylogenetic trees were constructed using MEGA 4.1 software with the neighbor-joining (NJ) algorithm.

2.4. Quantitative real time reverse transcription-PCR (qRT-PCR)

2.4.1. qRT-PCR analysis of WR-IL20, WCC-IL20 and RCC-IL20 expression in fish tissues under normal physiological conditions

Distal intestine, brain, kidney, liver, spleen, skin, gill and muscle were taken aseptically from WR, WCC and RCC (as described above, three fish in each experiment) and used for total RNA extraction with EZNA Total RNA Kit II (Omega Bio-tek, Doraville, CA, USA). The first-strand cDNAs were synthesized as described above. qRT-PCR was carried out in a 7500 Real-time PCR System (Applied Biosystems, Foster City, CA, USA) using the PowerUp SYBR Green Master Mix (Thermo Fisher Scientific). The qRT-PCR program was: 1 cycle of 50 °C/2 min, 1 cycle of 95 °C/2 min, 40 cycles of 95 °C/15 s, 56 °C/15s, 72 °C/35s, followed by dissociation curve analysis (60 °C–95 °C) to verify the amplification of a single product. The expression levels of *WR-IL20, WCC-IL20 and RCC-IL20* were analyzed using comparative threshold cycle method ($2^{-\Delta\Delta CT}$) with beta-actin (ACTB) as an internal reference [17]. The PCR primers were listed in Table S1. PCR efficiency (E) and correlation coefficient (R^2) were conducted as previously described [20]. The experiment was performed three times, each time with three fish.

2.4.2. qRT-PCR analysis of WR-IL20, WCC-IL20 and RCC-IL20 expression in fish tissues during bacterial infection

A. hydrophila CCL1 (MK014495), a bacterial pathogen isolated from diseased crucian carps [21], was cultured in Luria-Bertani broth (LB) medium at 28 °C to an OD$_{600}$ of 0.8; the cells were washed with PBS and
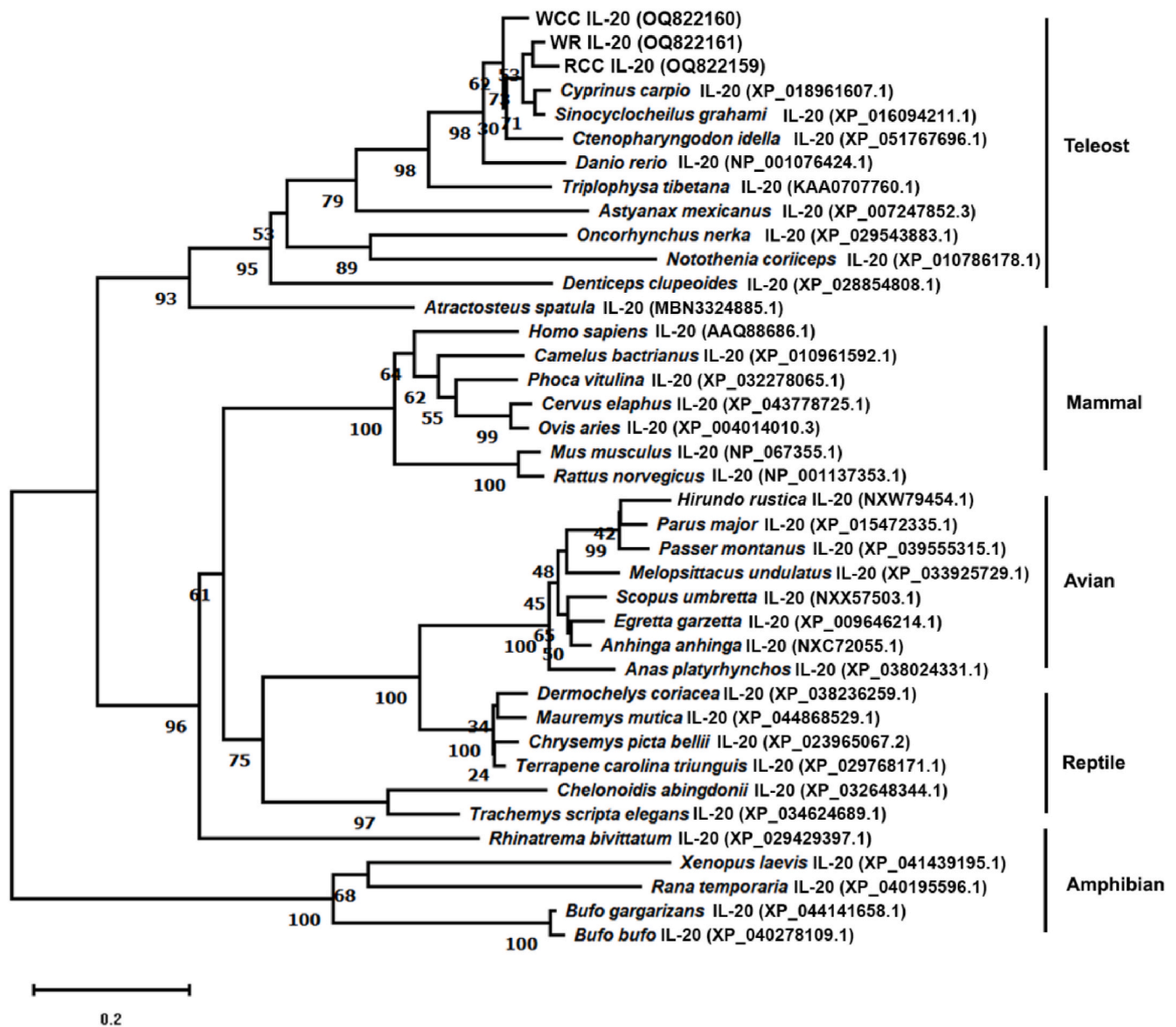
Fig. 3. Phylogenetic trees constructed with the amino acid sequences of IL-20 from the indicated species. The tree was constructed using the neighbor-joining (NJ) algorithm with the Mega 4.1 program based on multiple sequence alignment by Clustal X. Bootstrap values of 1000 replicates (%) were indicated for the branches.

resuspended in PBS to 1×10^5 CFU/ml. WR, WCC and RCC (as described above, three fish in each group) were divided randomly into two groups and injected intramuscularly (i.m.) with 100 μl A. *hydrophila* or PBS (control). Distal intestine, liver, spleen and kidney were taken from the fish (three at each time point) at 6, 12, 24 and 48 h post-bacterial infection (hpi). Total RNA extraction, cDNA synthesis, and qRT-PCR were performed as described above. The experiment was performed three times.

2.5. Plasmid construction

The protein expression vector pET259 was constructed as previously described [18]. To construct pEtWR-IL20, which expresses the extra-cellular region of WR-IL20 (rWR-IL20, residues 26 to 177), the coding sequence of WR-IL20 was amplified by PCR with primers IL20-F2 and IL20-R2 (Table S1); the PCR product was ligated with the T-A cloning vector pMD-18T vector (Takara, Dalian, China), and the recombinant plasmid was digested with EcoRV to retrieve the *WR-IL20*-containing

fragment, which was inserted into pET259 at the SwaI site, resulting in pEtWR-IL20.

2.6. Purification of recombinant proteins

Escherichia coli BL21 (DE3) (TransGen Biotech., Beijing, China) was transformed with pEtWR-IL20; the transformants were cultured in LB medium at 37 °C to mid-logarithmic phase, and isopropyl-β-D-thio-galactopyranoside was added to the culture to a final concentration of 0.4 mM. After growing at 24 °C for an additional 6 h, the cells were harvested by centrifugation, and His-tagged proteins were purified using Ni-NTA Agarose (Sangon Biotech., Shanghai, China, C600033) as rec-ommended by the manufacturer. The proteins were treated with Triton X-114 to remove endotoxin as reported previously [22]. The concen-trated proteins were analyzed by sodium dodecyl sulfate-polyacrylamide gel electrophoresis (SDS-PAGE) and visualized after staining with Coomassie brilliant blue R-250. The concentration of the proteins was determined using the Bradford method with bovine
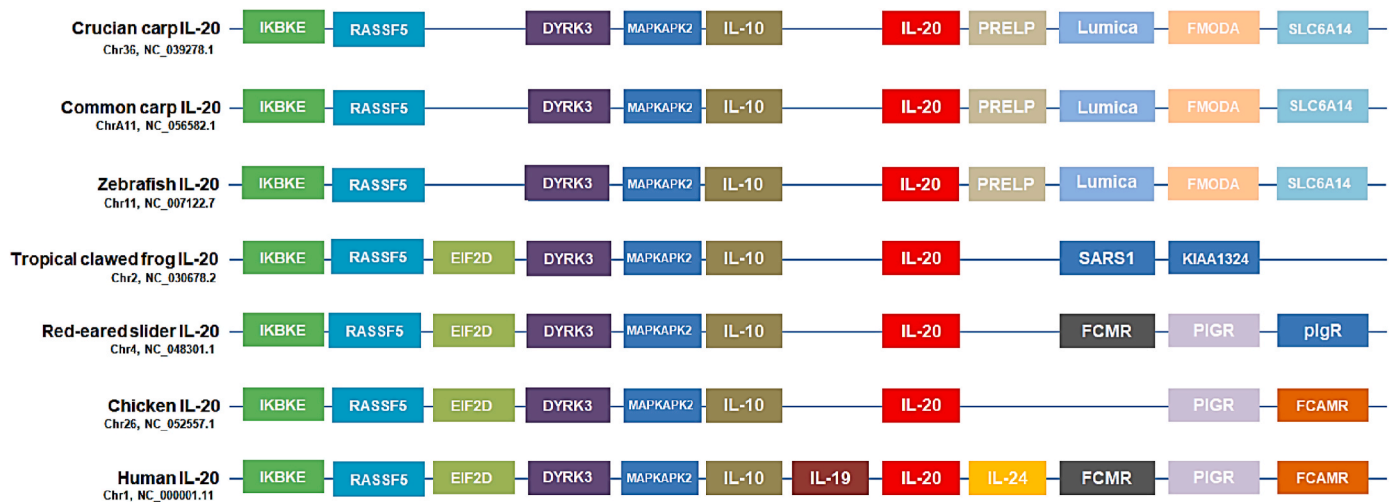
Fig. 4. Gene collinearity analyses within the crucian carp IL-20 and other vertebrates. The genes were indicated by rectangles to show their positions in the indicated genome.

serum albumin as the standard. After purification, the remaining endotoxin levels in the proteins were determined with limulus amebocyte lysate QCL-1000 kit (Lonza, Walkersville, USA) to ensure the endotoxin levels were less than 0.1 EU/ml in all purified proteins [23].

2.7. Leukocytes isolation

Head kidney leukocytes (HKL) were isolated from healthy WR, WCC and RCC (named WR-HKL, WCC-HKL and RCC-HKL, respectively) by Percoll density gradient centrifugation as previously described [9]. Briefly, head kidney tissues of healthy WR, WCC and RCC were collected and lightly ground in Leibovitz L-15 medium (Gibco) containing 10% fetal bovine serum (FBS, Gibco) before being filtered with nylon gauze. The Percoll (GE Healthcare) was mixed with 10 × PBS at a ratio of 9:1 and diluted to 34% and 52% (v/v) using L-15 medium, respectively. 4 ml 52% Percoll, 34% Percoll and head kidney cell suspension were added into a 15 ml centrifuge tube. After centrifugation at 500*g* with the lowest acceleration and deceleration at room temperature for 35 min, leukocytes located between 34% and 52% Percoll were collected and washed twice with L-15 medium for further experiments.

2.8. Lymphocytes stimulation

Isolated WR-HKL, WCC-HKL and RCC-HKL were cultured in DMEM complete medium (10% FBS and 1% penicillin-streptomycin). Firstly, WR-HKL, WCC-HKL and RCC-HKL were incubated in sterile PBS at 28 °C for 30 min. Then, 1×10^7 lymphocytes were stimulated with 5 μg/mL rWR-IL20 or sterile PBS (control) for 12 h according to a previous study [24], respectively. After the reaction was terminated by precooling sterile PBS, stimulated cells and control stimulated cells were collected by centrifugation. Total RNA and cDNA were then prepared as described above. qRT-PCR was used to analyze the expressions of *c-Myc*, *cyclin-D*, *Bcl-2*, *JAK1*, *TYK2* and *STAT3* as above. The PCR primers were listed in Table S1. The transcripts of qRT-PCR were sequenced to verify the specificity of the primers as described in our previous study [9]. The experiment was performed three times.

2.9. Statistical analysis

All experiments were performed in triplicate or independently for three times, and statistical analyses were carried out with GraphPad Prism 6 (GraphPad Software, San Diego, CA, USA). Data were analyzed with one-way analysis of variance (ANOVA) with Kruskal-Wallis' comparison, and statistical significance was defined as $P < 0.05$. For the qRT-

PCR, the relative expressions are normalized via beta-actin (ACTB) expression before calculating the relative expression levels to PBS treatment.

3. Results

3.1. Multiple alignments

The deduced amino acid sequence of WR-IL20, WCC-IL20 and RCC-IL20 were both composed of 177 residues (Fig. 1). Sequence alignment showed that WR-IL20 shared 95.48% and 94.35% overall sequence identities with its parents RCC-IL20 and WCC-IL20 respectively. Moreover, in teleost species family, the WR-IL20 shared higher identities to IL-20 homologues from *Cyprinus carpio* (92.66%), *Sinocyclocheilus graham* (92.66%), *Ctenopharyngodon idella* (88.7%) and *Danio rerio* (83.73%), with moderate identities to *Triplophysa tibetana* (72.32%) and *Astyanax mexicanus* (64.52%), and lower identities to *Atractosteus spatula* (54.14%), *Oncorhynchus nerka* (51.79%) and *Denticeps clupeoides* (49.35%). The WR-IL20 also had relative low identities to mammalian IL-20s. The overall sequence identities between WR-IL20 and human IL-20 and house mouse IL-20 were 44.94% and 42.31%, respectively (Fig. 1). Besides, there were six well conserved cysteine residues amongst the fish IL-20 and mammalian IL-20 molecules (Fig. 1).

3.2. Structure characteristics

In order to identify whether there is a functional domain, we first performed the SMART analysis based on the WR-IL20, WCC-IL20 and RCC-IL20 protein sequences. *In silico* analysis identified a conserved IL-10 domain in WR-IL20, WCC-IL20 and RCC-IL20, which was evolutionarily conserved when compared with its homologues from zebrafish IL-20 and human IL-20 (Fig. 2A). To determine the structural changes of *IL-20* gene during evolution, we predicted and mapped the *IL-20* gene structure. It showed that the genomic sequences of *WR-IL20*, *WCC-IL20* and *RCC-IL20* possessed five exons and four introns, which were the same in zebrafish IL-20 and human IL-20 (Fig. 2B). More importantly, according to tertiary structure prediction, WR-IL20, WCC-IL20 and RCC-IL20 were composed of multiple similar β-stands with zebrafish IL-20 and human IL-20 (Fig. 2C).

3.3. Phylogenetic analysis

To further explore the evolutionary relationship between WR-IL20 and its congeners in other species, a phylogenetic tree was constructed
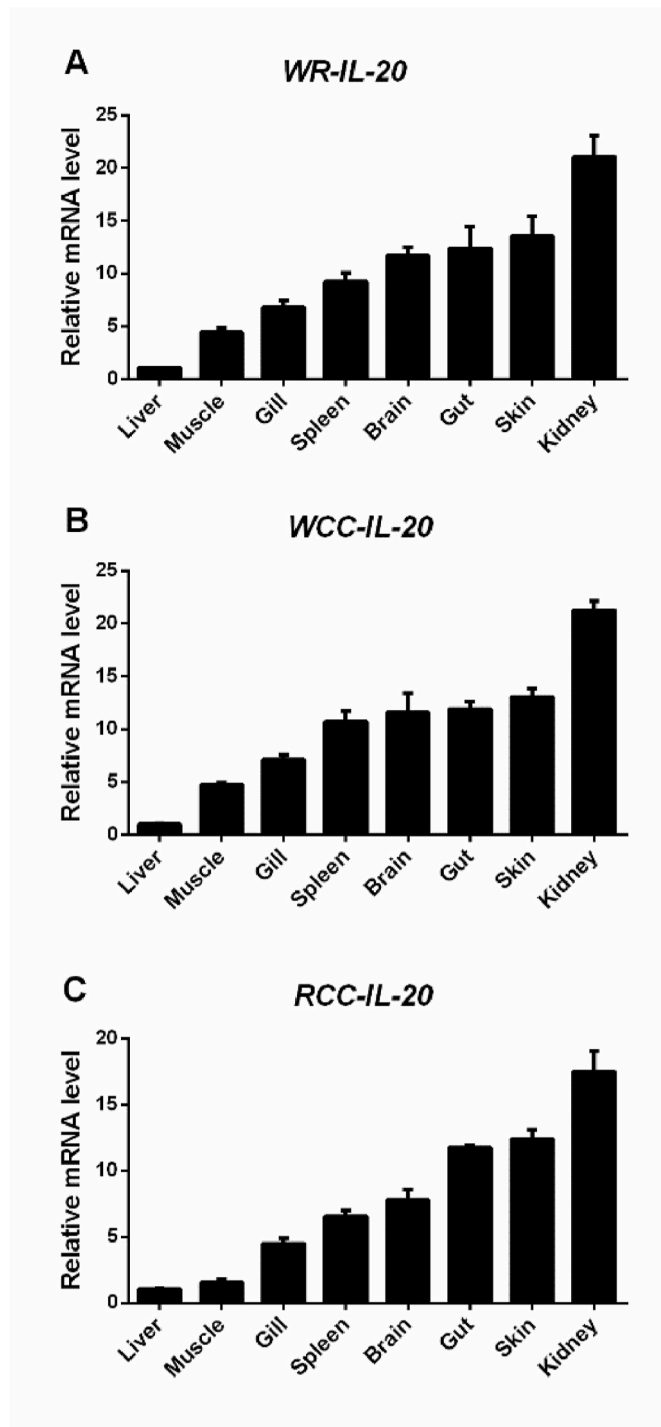
Fig. 5. WR-IL20, WCC-IL20 and RCC-IL20 expressions in fish tissues under normal physiological condition. Tissues from WR, WCC and RCC including distal intestine, brain, kidney, liver, spleen, skin, gill and muscle were sampled and the expressions of WR-IL20 (A), WCC-IL20 (B) and RCC-IL20 (C) in indicated tissues were determined by quantitative real time RT-PCR, respectively. For convenience of comparison, the expression level in liver was set as 1.

using neighbor joining algorithm based on multiple sequence alignment. The WR-IL20 firstly clustered with WCC-IL20, RCC-IL20 and common carp IL-20, and then clustered with the same molecules from other teleost, suggesting a close relationship of WR-IL20 with its homologues from teleost (Fig. 3). The IL-20 from other vertebrates, such as amphibian, reptile, avian and mammal, formed sister groups of the group formed by teleost IL-20 (Fig. 3).

3.4. Synteny characterization

As revealed by the genome-wide identification in the NCBI GenBank database, crucian carp possessed an *IL-20* gene on chromosome 36 (https://www.ncbi.nlm.nih.gov/nuccore/NC_039278.1). The neighboring genes of *IL-20* among different vertebrates were analyzed by comparative genomics. Both bony fish IL-20s and its homologues from other vertebrates including tropical clawed frog, red-eared slider and chicken were located in a chromosomal fragment composed of *DYRK3-MAPKAPK2-IL10-IL20* genes (Fig. 4). However, the upstream gene and downstream gene of *IL-20* in human were *IL-19* and *IL-24* respectively. In addition, the *IL-24* downstream of human *IL-20* was replaced by PRELP when it evolved into bony fish (Fig. 4). In summary, the results of phylogenetic status, collinearity, exon-intron composition, tertiary structure and functional motif indicated that WR-IL20 was relatively conserved in the evolutionary process, suggesting that crucian carp IL-20 may have similar functions to IL-20 in higher vertebrates.

3.5. mRNA expression under normal physiological conditions

qRT-PCR analysis showed that under normal physiological conditions, WR-IL20 expression was detected, in increasing order, in the immune-related tissues including liver, muscle, gill, spleen, brain, distal gut, skin and kidney (Fig. 5A). Moreover, qRT-PCR analysis was also conducted to examine the expressions of the WCC-IL20 and RCC-IL20 under normal physiological conditions in immune-related tissues (brain, gill, heart, spleen, muscle, kidney, intestine and liver). The results showed that the expressions of WCC-IL20 and RCC-IL20 were detected in all examined tissues, and had similar expression patterns to WR-IL20 (Fig. 5B and C). The wide distributions of WR-IL20, WCC-IL20 and RCC-IL20 in immune-related tissues suggested that they might be involved in the immune response of crucian carp.

3.6. mRNA expression in the presence of A. hydrophila infection

To establish the involvement of WR-IL20 in immune responses during bacterial infection, WR were infected with *A. hydrophila* and the dynamics changes of WR-IL20 transcript levels in the distal gut, kidney, liver and spleen were monitored. The results showed that significant inductions of WR-IL20 expression were detected in distal gut and kidney at 12 and 24 hpi, with the highest level of induction occurring at 12 hpi (Fig. 6A and D). In liver and spleen, compared with control groups, the mRNA levels of WR-IL20 were significantly induced at 12 and 24 hpi, with the highest level of induction occurring at 24 hpi (Fig. 6G and J). Furthermore, to examine the expression patterns of IL-20 in the parents of WR upon bacterial infection, WCC and RCC were challenged experimentally with *A. hydrophila* respectively. At 6, 12, 24 and 48 hpi, the expressions of WCC-IL20 and RCC-IL20 in the distal gut, kidney, liver and spleen of the infected fish were determined by qRT-PCR. The results showed that WCC-IL20 and RCC-IL20 had the same expression patterns to WR-IL20 after bacterial infection (Fig. 6B–J). In conclusion, these results indicated that IL-20 was involved in the immune response in crucian carp during bacterial infection.

3.7. WR-IL20 enhances the activation of the JAK1/STAT3 pathway

To investigate the immune function of WR-IL20, we prepared the recombinant WR-IL20 protein (rWR-IL20) using a prokaryotic expression system and rWR-IL20 was then purified from *E. coli* as a His-tagged protein (Fig. 7). Subsequently, we used this high-purity and soluble rWR-IL20 to subsequent experiments. To further confirm the immune function of WR-IL20 on crucian carp, the head-kidney leukocytes from WR (WR-HKL), WCC (WCC-HKL) and RCC (RCC-HKL) were prepared respectively. We next stimulated the WR-HKL, WCC-HKL and RCC-HKL with rWR-IL20 and examined the activation of the classical JAK1/STAT3 pathway respectively. Firstly, compared to the control group,
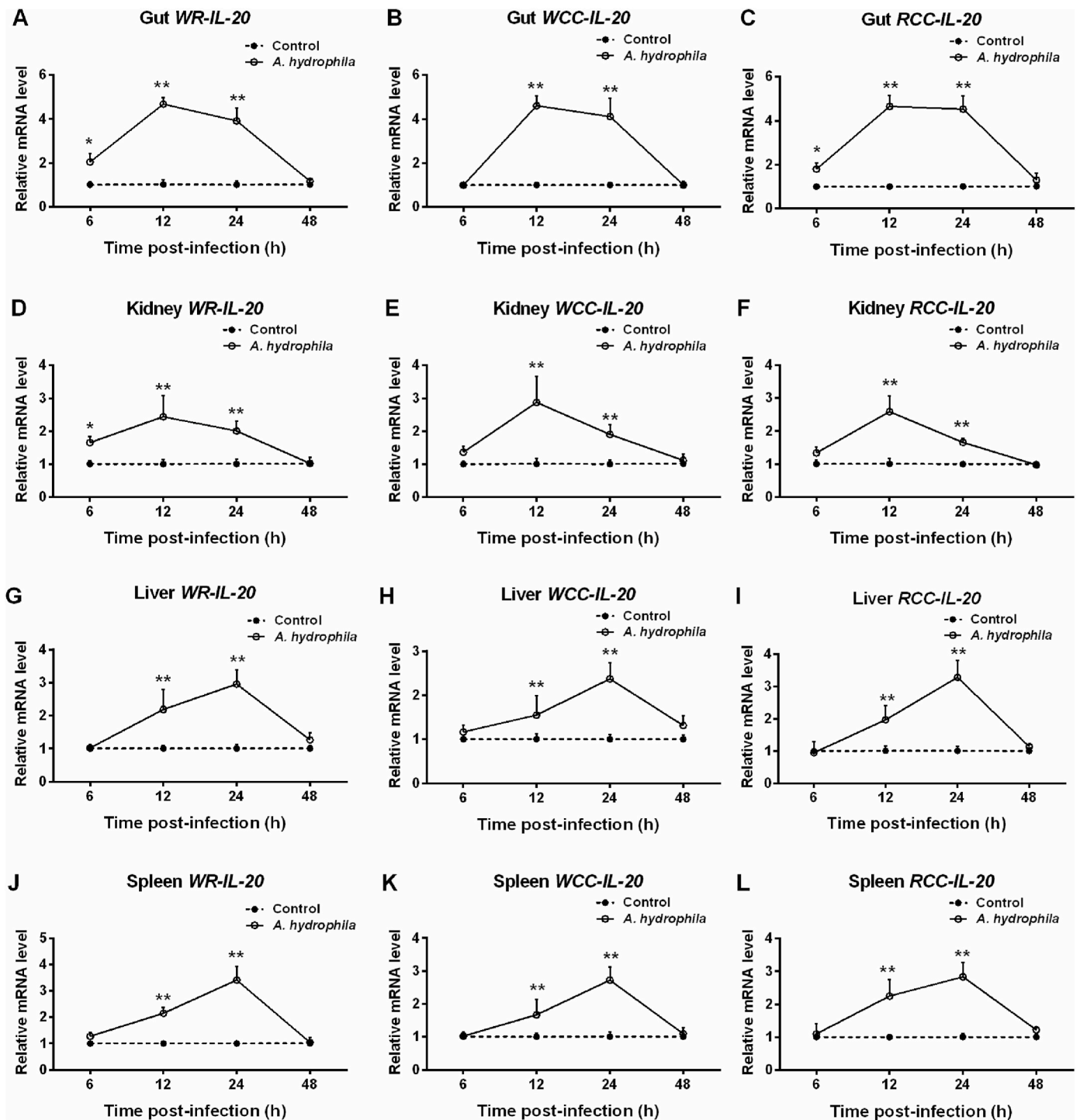
Fig. 6. WR-IL20, WCC-IL20 and RCC-IL20 expressions in fish tissues under bacterial infection condition. WR, WCC and RCC were infected with or without (control) *Aeromonas hydrophila*, and WR-IL20, WCC-IL20 and RCC-IL20 expressions in distal intestine, kidney, liver and spleen were determined by quantitative real time RT-PCR at various time points. In each case, the expression level of the control fish was set as 1. Values are shown as means ± SEM (N = 3). N, the number of times the experiment was performed. **$P < 0.01$.

rWR-IL20 stimulation both increased the mRNA expression of *c-Myc* and *cyclin-D* in WR-HKL, WCC-HKL and RCC-HKL respectively (Fig. 8A and B), indicating the potential capacity of WR-IL20 in promoting lymphocyte proliferation. Meanwhile, the anti-apoptotic gene *Bcl-2* was significantly up-regulated compared with the control groups (Fig. 8C), suggesting its potential roles in maintaining lymphocyte survival. Next, the activation of classical JAK1/STAT3 axis was examined at transcription levels. The results showed that administration of head kidney lymphocytes with rWR-IL20 enhanced the expressions of *JAK1, TYK2* and *STAT3* significantly in WR-HKL (Fig. 8D–F), suggesting that WR-IL20 may utilize an evolutionarily conserved JAK1/STAT3 axis to mediate subsequent immune function. Interestingly, it seemed that the responses of WR-HKL upon rWR-IL20 stimulation were higher than that of WCC-HKL and RCC-HKL, suggesting that this may be related to WR's stronger disease resistance, but further experiments are needed.
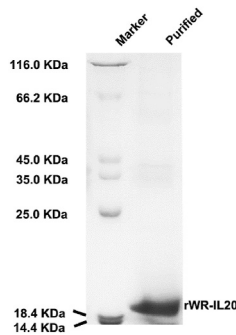
Fig. 7. SDS-PAGE analysis of rWR-IL20. Purified rWR-IL20 was analyzed by SDS-PAGE and viewed after staining with Coomassie brilliant blue R-250.

4. Discussion

The IL-10 family of cytokines consists of nine members: IL-10, IL-19, IL-20, IL-22, IL-24, IL-26, IL-28A, IL-28B, and IL-29 [1]. Among these cytokines, IL-19, IL-20, IL-22, IL-24, and IL-26 are belonging to IL-20 subfamily [1,2]. The IL-20 subfamily of cytokines primarily acts on various epithelial cells and protects these cells from invasion by extracellular pathogens [2]. In addition, IL-20 subfamily cytokines enhance tissue remodeling and wound-healing activities, which help to maintain tissue integrity and restore homeostasis of epithelial layers during infection and inflammatory responses [6,25–27]. However, how the IL-20 mediates immune defense in early vertebrates remains largely unknown.

In the present work, we cloned the sequence of IL-20 from *Carassius cuvieri* × *Carassius auratus* red var. (named WR-IL20) and its parents (named WCC-IL20 and RCC-IL20), respectively. Sequence alignment showed that WR-IL20 was slightly different from the parents WCC-IL20 and RCC-IL20, respectively. This is probably white crucian carp (WCC) and red crucian carp (RCC) are classified into different species in the genus of *Carassius* [28], thus the generation of WR by crossing of WCC and RCC is considered as interspecific hybridization. Although WR-IL20 was slightly different from the parent, SMART analysis showed that WR-IL20, WCC-IL20 and RCC-IL20 both had highly conserved IL-10 domains, and shared highly similarities of structure with its
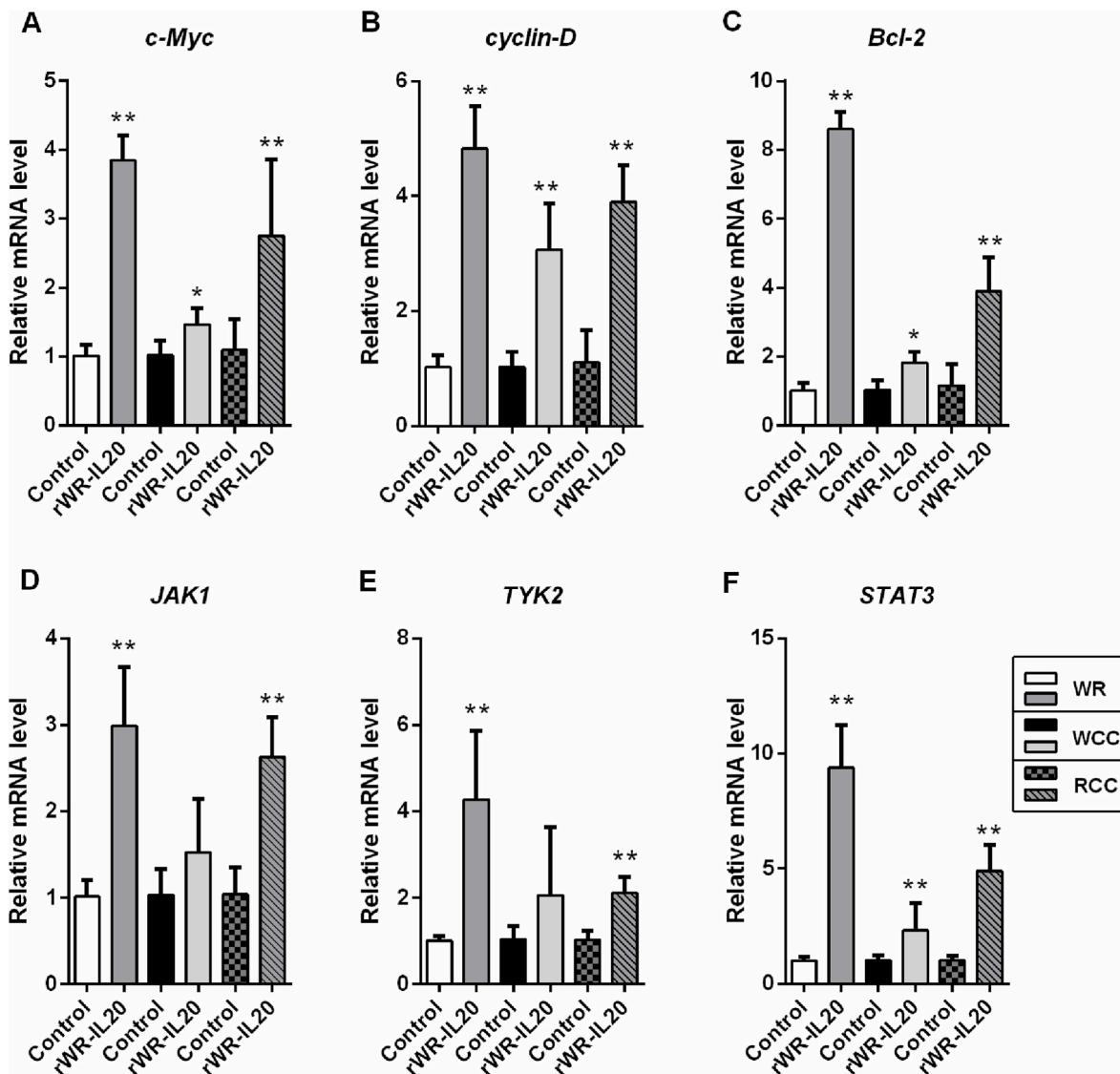

Fig. 8. Activation of downstream signaling pathway after WR-IL20 stimulation. Head kidney leukocytes from WR, WCC and RCC were treated with or without (control) rWR-IL20 for 12 h respectively, and *c-Myc* (A), *cyclin-D* (B), *Bcl-2* (C), *JAK1* (D), *TYK2* (E) and *STAT3* (F) expressions were determined by quantitative real time RT-PCR. For convenience of comparison, the expression levels of control groups were set as 1. Values are shown as means ± SEM (N = 3). N, the number of times the experiment was performed. *$P < 0.05$. **$P < 0.01$.

homologues zebrafish IL-20 and human IL-20. Moreover, the results of blast and phylogenetic analysis showed that WR-IL20, WCC-IL20 and RCC-IL20 had the higher identities to IL-20 from mammals, indicating that crucian carp IL-20 was evolutionarily conserved.

In human and crucian carp, IL-20 protein both had 176 amino acids (aa) with six conserved cysteine residues required for the characteristic α-helical secondary structure [11]. Besides, human IL-20 gene was located near the IL-10, IL-19, IL-24 genes within a 145 kb region on chromosome [8,29], while in crucian carp, IL-10 and IL-20L genes were found in the IL-10 locus, which contrasted with the presence of IL-10, IL-19, IL-20 and IL-24 in the corresponding locus in mammals. The five exons of most of vertebrate IL-20 were separated by four introns, but the gene structure of the multi-exon-intron had been maintained throughout evolution. These observations suggested that crucian carp IL-20 may share a common origin with IL-10.

In mammals, IL-20 was expressed by different cells and tissues but primarily by epithelial cells and myeloid cells such as monocytes, dendritic cells (DCs) and granulocytes [30]. In fish, the grass carp IL-20L was constitutively expressed in tissues and the highest expression level was detected in the head kidney [11,12]. Consistently, in our study, WR-IL20, WCC-IL20 and RCC-IL20 expressions were found to be relatively higher in the head kidney, which was considered as the major immune tissue in fish and accommodated a variety of immune cells including myeloid cells and lymphocytes. Interestingly, broad expression profiles of WR-IL20, WCC-IL20 and RCC-IL20 were both found in tissues including skin, gut and gill, suggesting that crucian carp IL-20 was a pleiotropic cytokine which may be required for the function of epithelial cells in tissue homeostasis.

In grass carp, there was an increase in the expression of the IL-20 at 24 h after infection *Flavobactrium columnare* [11,12]. In rainbow trout, the increased expression of IL-20L was only detected at late stages (4–24 h) of LPS stimulation in RTS-11 cells and in spleen 24–72 h after infection with *Yersinia ruckeri* [13]. Similarly, in this study, experimental infection with a bacterial pathogen *A. hydrophila* caused significant induction of WR-IL20 expression at 12–24 h in the intestine, head kidney, liver and spleen, indicating the increased expression of WR-IL20 by infection may be via the rapid increase of pro-inflammatory cytokines (e.g., IL-1b) and is involved in innate immune regulation in teleost. Moreover, similar expression profiles of WCC-IL20 and RCC-IL20 were also found in these tissues, suggesting that crucian carp IL-20 may perform similar functions to higher vertebrates.

IL-10 family cytokines activate the JAK/STAT signaling pathway, and STAT3 is the key downstream transcription factor used by IL-20 subfamily cytokines [1]. It has been proved that STAT3 up-regulates multiple functional genes related to proliferation and survival, including c-Myc, cyclin D1/D2, Bcl-XL, Bcl-2 and p53 [2]. In this study, we revealed that rWR-IL20 promoted significant up-regulation of *c-Myc*, *cyclin D* and *Bcl-2* genes in WR-HKL. In addition, the expressions of *JAK1*, *TYK2* and *STAT3* were also significantly increased in WR-HKL after rWR-IL20 stimulation. These results suggest that IL-20/JAK1/STAT3 signaling may take part in the lymphocyte response of crucian carp by promote cellular survival and proliferation. Interestingly, the expression of JAK1/STAT3 in WCC-HKL upon rWR-IL20 stimulation appears to be lower than that of RCC-HKL, while WR-HKL showed the strongest response to rWR-IL20 stimulation, which may be related to WR's stronger disease resistance. The reason may be that WR-IL20 may have a higher affinity to receptors than its parents, but further verification experiments are needed.

In conclusion, we identified a conserved cytokine IL-20 in WR, and we compared the differences of phylogenetic status, collinearity, exon-intron composition, tertiary structure, and functional motif between WR-IL20 and its parents. Bacterial infection resulted in increases in IL-20 expression in WR and its parents. In addition, WR-IL20 may enhance the response of JAK1/STAT3 axis, a classical signal pathway, to promote proliferation and anti-apoptosis ability of lymphocytes. This study may enrich our current knowledge regarding lymphocyte

response, and provide useful insights into the evolution of the innate immune system.

Author contributions

ZZ conceived and designed the experiments. QZ, NH, ZL and YY performed the experiments. QZ and ZZ analyzed the data. QZ and ZZ wrote and reviewed the manuscript. ZZ supervised the research. All authors contributed to the article and approved the submitted version.

Funding

Conflict of interest

The authors declare that the research was conducted in the absence of any commercial or financial relationships that could be construed as a potential conflict of interest.

Declaration of competing interest

The authors declare that they have no known competing financial interests or personal relationships that could have appeared to influence the work reported in this paper.

Appendix A. Supplementary data

Supplementary data to this article can be found online at https://doi.org/10.1016/j.repbre.2023.06.002.

References

[1] W. Ouyang, S. Rutz, N.K. Crellin, P.A. Valdez, S.G. Hymowitz, Regulation and functions of the IL-10 family of cytokines in inflammation and disease, Annu. Rev. Immunol. 29 (2011) 71–109.

[2] S. Rutz, X. Wang, W. Ouyang, The IL-20 subfamily of cytokines–from host defence to tissue homeostasis, Nat. Rev. Immunol. 14 (2014) 783–795.

[3] Z. Zhou, M. Ding, L. Huang, G. Gilkeson, R. Lang, W. Jiang, Toll-like receptor-mediated immune responses in intestinal macrophages; implications for mucosal immunity and autoimmune diseases, Clin. Immunol. 173 (2016) 81–86.

[4] L. Persaud, D. De Jesus, O. Brannigan, M. Richiez-Paredes, J. Huaman, G. Alvarado, L. Riker, G. Mendez, J. Dejoie, M. Sauane, Mechanism of action and applications of interleukin 24 in immunotherapy, Int. J. Mol. Sci. 17 (2016) 869.

[5] C. Eidenschenk, S. Rutz, O. Liesenfeld, W. Ouyang, Role of IL-22 in microbial host defense, Curr. Top. Microbiol. Immunol. 380 (2014) 213–236.

[6] J.H. Niess, P. Hruz, T. Kaymak, The Interleukin-20 cytokines in intestinal diseases, Front. Immunol. 9 (2018) 1373.

[7] S. Ni, F. Shan, J. Geng, Interleukin-10 family members: biology and role in the bone and joint diseases, Int. Immunopharm. 108 (2022), 108881.

[8] U.M. Wegenka, IL-20: biological functions mediated through two types of receptor complexes, Cytokine Growth F. R. 21 (2010) 353–363.

[9] X. Jiao, K. Li, M. Geng, K. Li, W. Liang, J. Zhang, Q. Zhang, H. Gao, X. Wei, J. Yang, Activated T cells are the cellular source of IL-22 that enhances proliferation and survival of lymphocytes in Nile tilapia, Fish Shellfish Immunol. 128 (2022) 216–227.

[10] X. Qiu, M. Lv, X. Jian, D. Chen, H. Zhou, A. Zhang, X. Wang, In vitro characterization of grass carp (*Ctenopharyngodon idella*) IL-26 in regulating inflammatory factors, Fish Shellfish Immunol. 66 (2017) 148–155.

[11] Z. Hassan, J. Wang, Y. Qin, W. Wang, Q. Liu, L. Lei, Z. Sun, Y. Yang, K. Wu, X. Zhu, Z. Wang, H. Feng, J. Zou, Functional characterization of an interleukin 20 like homologue in grass carp *Ctenopharyngodon idella*, Fish Shellfish Immunol. 115 (2021) 43–57.

[12] H. Dang, Z. Hassan, Z. Jia, Y. Wu, H. Xiao, W. Huang, X. Guo, X. Zhao, Y. Li, J. Zou, J. Wang, Grass carp IL-20 binds to IL-20R2 but induces STAT3 phosphorylation via IL-20R1, Fish Shellfish Immunol. 132 (2023), 108445.

[13] T. Wang, P. Díaz-Rosales, S.A. Martin, C.J. Secombes, Cloning of a novel interleukin (IL)-20-like gene in rainbow trout *Oncorhynchus mykiss* gives an insight into the evolution of the IL-10 family, Dev. Comp. Immunol. 34 (2010) 158–167.

[14] D. Aggad, C. Stein, D. Sieger, M. Mazel, P. Boudinot, P. Herbomel, J.P. Levraud, G. Lutfalla, M. Leptin, In vivo analysis of Ifn-γ1 and Ifn-γ2 signaling in zebrafish, J. Immunol. 185 (2010) 6774–6782.

[15] G. Lutfalla, H. Roest Crollius, N. Stange-Thomann, O. Jaillon, K. Mogensen, D. Monneron, Comparative genomic analysis reveals independent expansion of a lineage-specific gene family in vertebrates: the class II cytokine receptors and their ligands in mammals and fish, BMC Genom. 4 (2003) 29.

[16] Z. Cui, X. Zhu, F. Zhao, D. Li, Y. Deng, A. Tan, Y. Lai, Z. Huang, H. Gong, Molecular identification and functional exploration of interleukin-20 in snakehead (*Channa argus*) involved in bacterial invasion and the proliferation of head kidney leukocytes, Fish Shellfish Immunol. 127 (2022) 623–632.

[17] Y. Tang, M. Feng, X. Zhu, J. Long, Z. Zhou, S. Liu, WR-GLP2, a glucagon-like peptide 2 from hybrid crucian carp that protects intestinal mucosal barrier and inhibits bacterial infection, Fish Shellfish Immunol. 122 (2022) 29–37.

[18] C. Feng, X. Liu, N. Hu, Y. Tang, M. Feng, Z. Zhou, *Aeromonas hydrophila* Ssp1: a secretory serine protease that disrupts tight junction integrity and is essential for host infection, Fish Shellfish Immunol. 127 (2022) 530–541.

[19] Y. Tang, X. Liu, C. Feng, Z. Zhou, S. Liu, Nicotinamide phosphoribosyltransferase (Nampt) of hybrid crucian carp protects intestinal barrier and enhances host immune defense against bacterial infection, Dev. Comp. Immunol. 128 (2022), 104314.

[20] C. Feng, Y. Tang, X. Liu, Z. Zhou, CMPK2 of triploid crucian carp is involved in immune defense against bacterial infection, Dev. Comp. Immunol. 116 (2021), 103924.

[21] Z. Zhou, C. Feng, X. Liu, S. Liu, 3nLcn2, a teleost lipocalin 2 that possesses antimicrobial activity and inhibits bacterial infection in triploid crucian carp, Fish Shellfish Immunol. 102 (2020) 47–55.

[22] Z.J. Zhou, L. Sun, CsCTL1, a teleost C-type lectin that promotes antibacterial and antiviral immune defense in a manner that depends on the conserved EPN motif, Dev. Comp. Immunol. 50 (2015) 69–77.

[23] C. Feng, X. Liu, Y. Tang, M. Feng, Z. Zhou, S. Liu, A novel ladderlectin from hybrid crucian carp possesses antimicrobial activity and protects intestinal mucosal barrier against *Aeromonas hydrophila* infection, Fish Shellfish Immunol. 124 (2022) 1–11.

[24] M. Geng, K. Li, K. Ai, W. Liang, J. Yang, X. Wei, Evolutionarily conserved IL-27β enhances Th1 cells potential by triggering the JAK1/STAT1/T-bet axis in Nile tilapia, Fish Shellfish Immunol Rep 4 (2023), 100087.

[25] M.S. Chang, Y.H. Hsu, The role of IL-20 in chronic kidney disease and diabetic nephropathy: pathogenic and therapeutic implications, J. Leukoc. Biol. 104 (2018) 919–923.

[26] T.W. Kragstrup, T. Andersen, L.D. Heftdal, M. Hvid, J. Gerwien, P. Sivakumar, P. C. Taylor, L. Senolt, B. Deleuran, The IL-20 cytokine family in rheumatoid arthritis and spondyloarthritis, Front. Immunol. 9 (2018) 2226.

[27] E. Caparrós, R. Francés, The interleukin-20 cytokine family in liver disease, Front. Immunol. 9 (2018) 1155.

[28] J. Luo, Y. Gao, W. Ma, X. Bi, S. Wang, J. Wang, Y. Wang, J. Chai, R. Du, S. Wu, A. Meyer, R. Zan, H. Xiao, R.W. Murphy, Y. Zhang, Tempo and mode of recurrent polyploidization in the *Carassius auratus* species complex (Cypriniformes, Cyprinidae), Heredity 112 (2014) 415–427.

[29] M.V. Autieri, IL-19 and other IL-20 family member cytokines in vascular inflammatory diseases, Front. Immunol. 9 (2018) 700.

[30] J.E. Beute, A.Y. Kim, J.J. Park, A. Yang, K. Torres-Shafer, D.W. Mullins, P. Sundstrom, The IL-20RB receptor and the IL-20 signaling pathway in regulating host defense in oral mucosal candidiasis, Front. Cell. Infect. Microbiol. 12 (2022), 979701.